

Effects Of Missing Atom Defect On The Mechanical Properties Of Black Phosphorene Nanotube

Van-Trang Nguyen

Department of Mechanical Design and Manufacture, Faculty of mechanical engineering, Thai Nguyen University of Technology, 3/2 street, Tich Luong ward, Thai Nguyen city, Vietnam

ABSTRACT:We investigate the effect of missing atom defect to the mechanical properties of black phosphorene nanotube (BPNT) through molecular dynamics finite element method with Stillinger-Weber potential. We found that effect of the defect on Young's modulus of phosphorene tube is insignificant. In contrast to, fracture stress and fracture strain of defective tube reduce up to 14% and 57%, respectively, compared with the pristine one. Simulation results will help to design and use BPNT for its future applications.

Keywords:Phosphorene, Mechanical properties, Missing atom defect.

Date Of Submission:12-10-2018

Date Of Acceptance: 27-10-2018

I. INTRODUCTION

Two-dimensional black phosphorous, namely, black phosphorene has been recently synthesis [1-5]. Black phosphorene is a semiconductor with a large direct band gap of 1.51 eV [6]. Black phosphorene has potential application in nanoelectronics, optoelectronics [2, 6, 7], gas sensors [8] and the anode material of Li-ion batteries [9, 10]. The pristine and defective armchair (0, 10) black phosphorene nanotube (BPNT) is studied. Defect is assumed to locate at tube's center.

The mechanical properties of pristine black phosphorene nanotube have been investigated clearly by density functional theory (DFT) calculations [11-14], density functional theory based finite element model (DFT-FEM)[15], density functional tight-binding (DFT-TB)[16], molecular dynamics simulations (MD)[17-21], molecular dynamics finite element method (MDFEM)[22-24]. However, effects of missing atom defect on the mechanical properties of black phosphorene nanotube have a little study. Liu et al.[25, 26] showed that missing atoms could reduce significantly the tensile performance of BPNTs. The fracture strength and strain of black phosphorene were reported to reduce about 23-50% and 40-66%, respectively by MD simulation[25].

The present work studies through molecular dynamics finite element method (MDFEM) the effect of a missing atom defect to the mechanical properties BPNTs under uniaxial tension. Since, the zigzag BPNT was found to have poorer stability than the

armchair BPNT [27]. Hence, only the armchair BPNT is considered in this study.

II. Framework for analysis

Stillinger-Weber potential is here used to model the P-P interatomic interactions[28]. The potential energy E of the atomic structure is the total of the bond stretching energy E_r and bond angle bending energy

E_θ :

$$E = E_r + E_\theta \quad (1)$$

$$E_r = \sum_{e=1}^M V_2, \quad E_\theta = \sum_{e=1}^N V_3 \quad (2)$$

$$V_2 = A e^{\left[\frac{\rho}{(r_{ij} - r_{\max ij})} \right]} \left(\frac{B}{r_{ij}^4} - 1 \right) \quad (3)$$

$$V_3 = K e^{\left[\frac{\rho_{ij}}{(r_{ij} - r_{\max ij})} + \frac{\rho_{ik}}{(r_{ik} - r_{\max ik})} \right]} \left(\cos \theta_{ijk} - \cos \theta_o \right)^2 \quad (4)$$

Where V_2 corresponds to the bond-stretching and V_3 associates with the angle-bending. M and N denote the total numbers of bond-stretching and angle-bending element, respectively (Fig. 1). Cutoffs $r_{\max ij}$, $r_{\max ik}$ are geometrically determined by the material's structure. A , K are energy parameters. ρ , B , ρ_{ij} , ρ_{ik} , θ_o are five geometrical parameters. r_{ij} , r_{ik} are length of ij and ik . θ_{ijk} is angle between bond ij and ik .

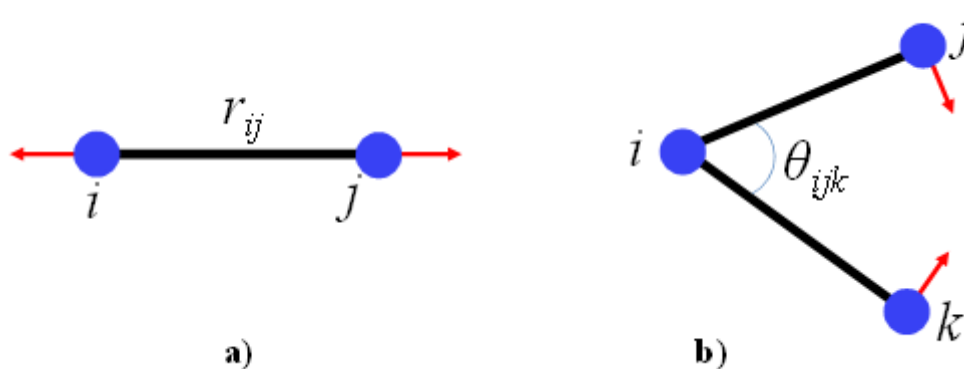


Fig. 1. Two element types used in MDFEM with Stillinger-Weber potential: a) Two-body (bond-stretching) element; and b) Three-body (angle-bending) element.

Stillinger-Weber potential parameters are taken from [28] for P-P interaction in black phosphorene and tabulated in table 1 and 2.

Table 1 Two-body (bond-stretching) Stillinger-Weber potential parameters

	A, nN.Å	ρ , Å	B, Å ⁴	r_o , Å	r_{maxij} , Å
P – P	5.7962	0.809	14.287	2.224	2.790

Table 2 Three-body (angle-bending) Stillinger-Weber potential parameters. P_t and P_b indicate the phosphorus atoms belonging to inner and outer tube diameter, respectively.

Typ es	K, nN.Å	θ_o , degre e	ρ_{ij} , Å	ρ_{ik} , Å	r_{maxij} , Å	r_{maxik} , Å	r_{maxjk} , Å
P _t – P _t	57.068	96.35	8	0.809	2.79	2.79	3.89
P _b – P _b	57.068	96.35	8	0.809	2.79	2.79	3.89
P _t – P _b	51.162	102.0	8	0.809	2.79	2.79	3.89
P _b – P _t	51.162	102.0	8	0.809	2.79	2.79	3.89

While density functional theory (DFT) calculations and molecular dynamics (MD) simulations are time-consuming, molecular dynamic finite element methods (MDFEM), sometime known as atomic-scale finite element methods or atomistic finite element methods, have been developed to analyze nanostructured materials in a computationally efficient way, see e. g. [29, 30]. To

achieve the atomic positions of the BPNT under specific boundary conditions, molecular dynamic finite element method (MDFEM) is here adopted. In MDFEM, atoms and atomic displacements are considered as nodes and translational degrees of freedom (nodal displacements), respectively. Both first and second derivatives of system energy are used in the energy minimization computation, hence it is faster than the standard conjugate gradient method which uses only the first order derivative of system energy as discussed in [29]. The stiffness matrices of these elements are established based upon interatomic potentials. Similar to conventional finite element method, global stiffness matrix is assembled from element stiffness matrices. Hence, relations between atomic displacement and force can be derived by solving a system of equations. Molecular dynamics finite element method (MDFEM) with Stillinger-Weber potential is used to simulate the uniaxial compression and tension of BPNT [22-24]. σ and ϵ are the nominal axial stress (engineering stress) and nominal axial strain (engineering strain), respectively. Young's modulus Y is determined from the first derivative of the stress-strain curve at strain $\epsilon=0$. Due to an ambiguous value of the tube's thickness t, we use the product Yt and σt to denote 2D Young's modulus and 2D stress, respectively. Pristine and defective (0, 10) armchair BPNT is considered.

III. RESULTS AND DISCUSSION

Fig.2 shows the stress-strain curves of pristine and defective (0, 10) armchair BPNT under

uniaxial tension. The axial stress increases monotonously with the rising of the axial strain up to a peak value, then the stress drops suddenly as shown in Fig. 2. Hence, maximal axial stress and strain at maximal stress refer to fracture stress and fracture strain, respectively.

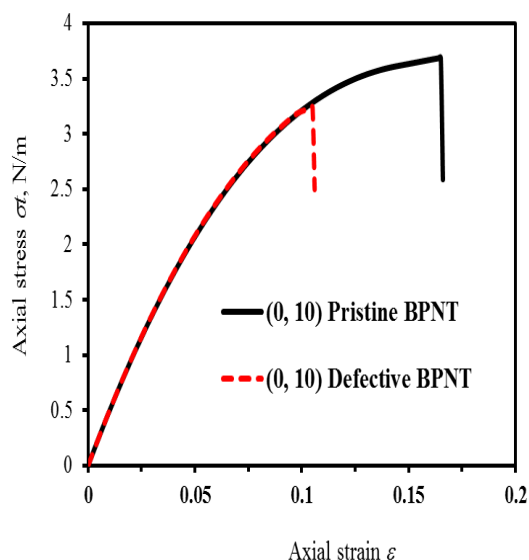


Fig. 2. The stress-strain curves of pristine and defective (0, 10) armchair BPNT under uniaxial tension

Table 3 shows the Young's modulus, fracture stress and fracture strain of pristine and defective (0, 10) armchair BPNT under uniaxial tension.

Table 3 Mechanical properties of pristine and defective (0, 10) armchair BPNT under uniaxial tension

Armchair nanotube	Young's modulus Yt, N/m	Fracture stress σ_t , N/m	Fracture strain ϵ , %
(0, 10) pristine	51.68	3.689	16.5
(0, 10) defective	51.93	3.243	10.5

The results show that the defective tube exhibit almost the same Young's modulus as the pristine one as indicated in Table 3. Therefore, the defect has almost no effect on Young's moduli of phosphorene tube. In contrast, the defect affects significantly on the fracture stress and strain. Due to a single defect in the tube's center, the fracture stress and fracture strain of defective tube reduce up to 14% and 57%, respectively, compared with the pristine one. Our results are in good agreement with those from MD simulations[25]. Fig. 3 shows snapshots of defective (0, 10) armchair BPNT under uniaxial tension.

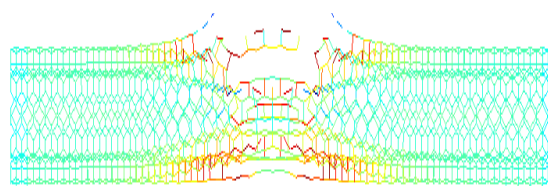


Fig. 3. shows snapshots of defective (0, 10) armchair BPNT under uniaxial tension.

ACKNOWLEDGEMENTS

Van-Trang Nguyen was supported by the Thai Nguyen University of Technology, Thai Nguyen University under grant number T2016-50.

REFERENCES

- [1]. Lu, W., et al., Plasma-assisted fabrication of monolayer phosphorene and its Raman characterization. *Nano Research*, 2014. **7**(6): p. 853-859.
- [2]. Li, L., et al., Black phosphorus field-effect transistors. *Nature nanotechnology*, 2014. **9**(5): p. 372-377.
- [3]. Xia, F., H. Wang, and Y. Jia, Rediscovering black phosphorus as an anisotropic layered material for optoelectronics and electronics. *Nature communications*, 2014. **5**: p. 4458.
- [4]. Reich, E.S., Phosphorene excites materials scientists. *Nature*, 2014. **506**(7486): p. 19.
- [5]. Kou, L., C. Chen, and S.C. Smith, Phosphorene: fabrication, properties, and applications. *The journal of physical chemistry letters*, 2015. **6**(14): p. 2794-2805.
- [6]. Qiao, J., et al., High-mobility transport anisotropy and linear dichroism in few-layer black phosphorus. *Nature communications*, 2014. **5**.
- [7]. Liu, H., et al., Phosphorene: an unexplored 2D semiconductor with a high hole mobility. *ACS Nano*, 2014. **8**(4): p. 4033-4041.
- [8]. Kou, L., T. Frauenheim, and C. Chen, Phosphorene as a superior gas sensor: selective adsorption and distinct I-V response. *The journal of physical chemistry letters*, 2014. **5**(15): p. 2675-2681.
- [9]. Guo, G.-C., et al., Pristine and defect-containing phosphorene as promising anode materials for rechargeable Li batteries. *Journal of Materials Chemistry A*, 2015. **3**(21): p. 11246-11252.
- [10]. Li, W., et al., Ultrafast and directional diffusion of lithium in phosphorene for high-performance lithium-ion battery. *Nano letters*, 2015. **15**(3): p. 1691-1697.
- [11]. Hu, T., Y. Han, and J. Dong, Mechanical and electronic properties of monolayer and bilayer phosphorene under uniaxial and isotropic

- strains. *Nanotechnology*, 2014. **25**(45): p. 455703.
- [12]. Wei, Q. and X. Peng, Superior mechanical flexibility of phosphorene and few-layer black phosphorus. *Applied Physics Letters*, 2014. **104**(25): p. 251915.
- [13]. Jiang, J.-W. and H.S. Park, Mechanical properties of single-layer black phosphorus. *Journal of Physics D: Applied Physics*, 2014. **47**(38): p. 385304.
- [14]. Hao, J., et al., Structure and elastic properties of black phosphorus nanotubes: A first-principles study. *physica status solidi (b)*, 2017. **254**(10).
- [15]. Ansari, R., A. Shahnazari, and S. Rouhi, A density-functional-theory-based finite element model to study the mechanical properties of zigzag phosphorene nanotubes. *Physica E: Low-dimensional Systems and Nanostructures*, 2017. **88**: p. 272-278.
- [16]. Sorokin, V. and Y. Zhang, Mechanical properties of phosphorene nanotubes: a density functional tight-binding study. *Nanotechnology*, 2016. **27**(39): p. 395701.
- [17]. Cai, K., et al., Strength and stability analysis of a single-walled black phosphorus tube under axial compression. *Nanotechnology*, 2016. **27**(27): p. 275701.
- [18]. Sha, Z.-D., et al., Mechanical properties and fracture behavior of single-layer phosphorene at finite temperatures. *Journal of Physics D: Applied Physics*, 2015. **48**(39): p. 395303.
- [19]. Yang, Z., J. Zhao, and N. Wei, Temperature-dependent mechanical properties of monolayer black phosphorus by molecular dynamics simulations. *Applied Physics Letters*, 2015. **107**(2): p. 023107.
- [20]. Le, M.-Q., Reactive molecular dynamics simulations of the mechanical properties of various phosphorene allotropes. *Nanotechnology*, 2018. **29**(19): p. 195701.
- [21]. Chen, W.-H., et al., Mechanical property assessment of black phosphorene nanotube using molecular dynamics simulation. *Computational Materials Science*, 2017. **133**: p. 35-44.
- [22]. Nguyen, V.-T. and M.-Q. Le, Atomistic simulation of the uniaxial compression of black phosphorene nanotubes. *Vietnam Journal of Mechanics*, 2018(DOI:10.15625/0866-7136/10982).
- [23]. Nguyen, V.-T. and L. Minh-Quy, Compressive buckling of black phosphorene nanotubes: An atomistic study. *Materials Research Express*, 2018.
- [24]. Nguyen, V.-T., D.-T. Nguyen, and L. Minh-Quy, Atomistic simulation of the uniaxial tension of black phosphorene nanotubes. *Vietnam Journal of Mechanics*, 2018.
- [25]. Liu, P., et al., Mechanical properties and fracture behaviour of defective phosphorene nanotubes under uniaxial tension. *Journal of Physics D: Applied Physics*, 2017. **50**(48): p. 485303.
- [26]. Liu, P., et al., Strength and buckling behavior of defective phosphorene nanotubes under axial compression. *Journal of Materials Science*, 2018. **53**(11): p. 8355-8363.
- [27]. Cai, K., et al., Thermal stability of a free nanotube from single-layer black phosphorus. *Nanotechnology*, 2016. **27**(23): p. 235703.
- [28]. Jiang, J.-W., Parametrization of Stillinger-Weber potential based on valence force field model: application to single-layer MoS₂ and black phosphorus. *Nanotechnology*, 2015. **26**(31): p. 315706.
- [29]. Liu, B., et al., The atomic-scale finite element method. *Computer Methods in Applied Mechanics and Engineering*, 2004. **193**: p. 1849-1864.
- [30]. Wackerfuß, J., Molecular mechanics in the context of the finite element method. *International Journal for Numerical Methods in Engineering*, 2009. **77**: p. 969-997.

Van-Trang Nguyen "Effects Of Missing Atom Defect On The Mechanical Properties Of Black Phosphorene Nanotube "International Journal of Engineering Research and Applications (IJERA) , vol. 8, no.10, 2018, pp 29-32